

Universal behavior in finite 2D kinetic ferromagnets

James Denholm* and Ben Hourahine†

*SUPA, Department of Physics, University of Strathclyde,
John Anderson Building, 107 Rottenrow, Glasgow G4 0NG. United Kingdom*

(Dated: September 3, 2022)

We show that quenching and coarsening of the kinetic Ising model with a non-conserved order parameter displays the same average evolution for finite systems of arbitrary size. This multiscale similarity applies not just within the characteristic length scale of the system, but also at all length and time scales, including in the regime where simple dynamical scaling fails for finite systems. As a consequence, beyond rapidly decaying finite size effects, the evolution of correlations in small systems exactly parallels arbitrarily larger cases. We suggest that dynamical scaling data collapse can be partially restored with an area law-like correction, but unlike the multiscale behavior, this does not hold for distances approaching a quarter of the system size.

PACS numbers: 64.60.De;64.75.Gh;05.50.+q

When a two-dimensional ferromagnet with a non-conserved order parameter is quenched from infinite to zero-temperature an elegant and beautiful phase separation process occurs: magnetic domains nucleate and coarsen until a dominant domain structure emerges that spans the system (see Fig. 1). This coarsening phenomena is found in the zero-temperature Glauber dynamics of the 2D Kinetic Ising magnet [1], which itself demonstrates a range of behaviors that have been extensively studied [2–4]. More generally, this same universal coarsening process has recently been shown to occur in systems as diverse as binary Bose gases and mutual killing in bacteria colony models [5–11].

The final result of quenching the nearest-neighbor Glauber Ising model to zero-temperature has also been shown to depend on the dimensionality of the system. In one spatial dimension the ground state is always reached [12] while in three dimensions the final states are a host of topologically complex configurations where the system is forever trapped in local energy minima [13–15]. In two dimensions, one not only finds that the ground state can be reached, but that the system can also become “frozen” into an on-axis striped phase or evolve through long-lived off-axis winding (diagonal) stripe configurations [15–18]. For nearest-neighbor interaction, these on-axis stripes are infinitely long-lived and the diagonal stripes eventually decay to homogeneity on a timescale that diverges with system size.

The probability of the system reaching these configurations is connected to the spanning probabilities of continuum percolation [17, 18], as demonstrated for a range of different lattice geometries [19, 20]. The ability to identify the “fate” of a quench early in its evolution is rooted in this connection to critical percolation and gives an understanding of how the system reaches its final configuration [16–18]. The scaling behavior of this “fate sealing” time has also been investigated on a variety of lattice geometries and boundary conditions [21]. The connection with continuum percolation has also been explored with

dynamical evolution rules other than Glauber dynamics [22]. More complex metastable behaviors can occur in 2D for longer range interactions [23].

The coarsening dynamics exhibited in the kinetic Ising model are generally thought to be well understood through the phenomenology of the dynamic scaling hypothesis. This describes coarsening in terms of the evolution of a single relevant process, the growth of a characteristic length scale [4], taken to be the typical domain size which governs the evolution of the (infinite sized) system. Despite its success, there are few systems where the validity of this hypothesis has been directly proven [24].

Interestingly, it has been shown that in the early phase of the Ising evolution there is another growing length scale, signifying the approach to critical percolation [20],

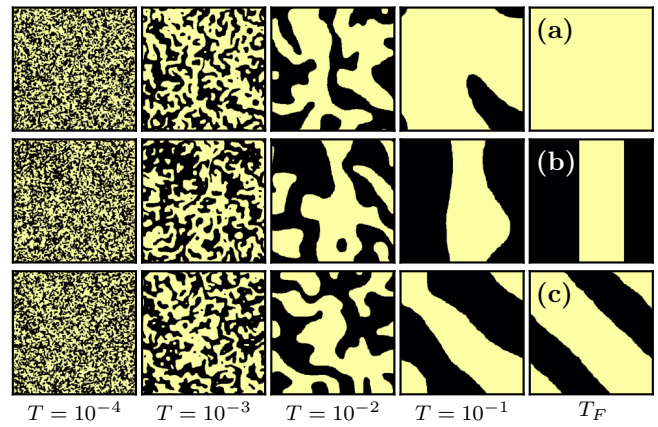


FIG. 1. Shows snapshots of zero-temperature coarsening from random initial conditions on square lattices of length $L = 2^{10}$ sites for quenches leading to (a) stable, (b) metastable and (c) long-lived diagonal stripe configurations. The last snapshots in the stable and metastable examples are the final states, which were reached at $T_F = 0.1680L^2$ and $T_F = 0.5734L^2$ respectively. The latter snapshot in the diagonal stripe case was halted early at $T_F = 10L^2$, illustrating the long lived nature of this configuration.

21, 25].

The cooperative nature of ferromagnets is such that their kinetic evolution can be captured with purely short range interactions, provided these decay rapidly with distance [18]. We accordingly consider nearest-neighbor interaction on square lattices of size $N = L^2$ sites in the absence of an external field. Spins are denoted by $\mathcal{S}_i = \pm 1$ and can be viewed as a binary mixture of phases with a non-conserved order parameter (or a non-conserved scalar field). The total energy of the system is given by the hamiltonian

$$\mathcal{H} = -\mathcal{J} \sum_{ij} \mathcal{S}_i \mathcal{S}_j, \quad (1)$$

where $\mathcal{J} > 0$ is a ferromagnetic coupling constant and j indexes the nearest neighbors of each spin \mathcal{S}_i . In accordance with zero-temperature Glauber dynamics, single spin flip events are sampled randomly with individual probabilities of 1 and 0.5 for energy decreasing or conserving events respectively [1]. Events that would incur an energy cost are forbidden (probabilities of 0). Physical time is advanced using the updates of Ref. [26] (also see Supplemental Material [27]).

Converged ensembles of 10^4 quench trajectories are obtained at a variety of lattice sizes for sizes $L = 2^n$ such that $2^5 \leq L \leq 2^{10}$. Each simulation is initialized with a different random microstate in order to mimic an infinite temperature configuration. The quenches are then categorized as cases evolving to stable final states, metastable final states or quenches that evolve through the long-lived diagonally wound stripe configurations. Each of these are then each considered as separate categories of quench. The scaling of the quench time when the system falls into the long-lived stripe configuration is greater than $\mathcal{O}(L^2)$, therefore we identify and discard these rare (occurrence probability of ≈ 0.04 [18]) trajectories.

From each category of quench trajectory we extract two-point same-time correlation functions from spins separated by specified distances $R = |\vec{R}_i + \vec{R}_j|$ in on-axis directions, obtaining expectations of the form

$$\mathcal{C}(R, t) = \langle \mathcal{S}_i(\vec{R}_i) \mathcal{S}_j(\vec{R}_i + \vec{R}_j) \rangle, \quad (2)$$

where the averaging is over each spin in the system, the four on-axis $\pi/2$ rotations of $\vec{R}_i + \vec{R}_j$ and across the ensemble of simulations. Due to the irregular time step and duration of each quench, time is normalized by the respective quench time T_q , i.e. $t = T/T_q$. Due to the stochastic time step, the data is linearly interpolated [28] to provide a regular time scale for averaging over simulations. Correlations are taken at all n such that $1 \leq R \leq L/2$ for $R = 2^n$. We then seek to compare the expectations of the correlations at different fractions of the system size, $r = R/L$, in normalized time, t . Our simulations were performed for geometries with both periodic and open boundary conditions, our conclusions

hold for both but for ease of presentation we show data for the periodic case only (see [27] for the open case).

The expectation value of the correlation function, Eq. (2), is unity (zero) for ferromagnetically ordered (disordered) configurations. At early times short range correlations are established, and as the quench progresses long range correlations emerge signifying the presence of large domain structures. Fig. 2a) shows the evolution of the correlation expectations averaged over an ensemble of quenches to homogeneous final states for a range of lattice sizes. The fractional distance at which correlations are compared for different lattice sizes is denoted by

$$F_L = \log_2 (R/L) = \log_2 (r), \quad (3)$$

where for example, $F_L = -1$ corresponds to half of the system length. As the system transitions from disorder to homogeneous order, the correlation progresses from 0 to 1. For striped quenches the behavior of the correlation function is similar, however the final configuration does not reach an expectation of 1 as there is always a remaining stripe of the minority phase. The final value of the correlation expectation in the case of these metastable final states depends upon the separation at which correlations are measured as well as the distribution of stripe widths across the ensemble. Long range correlations are more likely to involve spins on either side of a domain boundary, and therefore reduce the final value of the expectation. This behavior is seen in Fig. 2b), where the correlations expectations obtained across an ensemble of metastable final state quenches are shown. Fig. 2 demonstrates that at a fixed fraction of the system size, the same evolution is occurring for systems of any size when

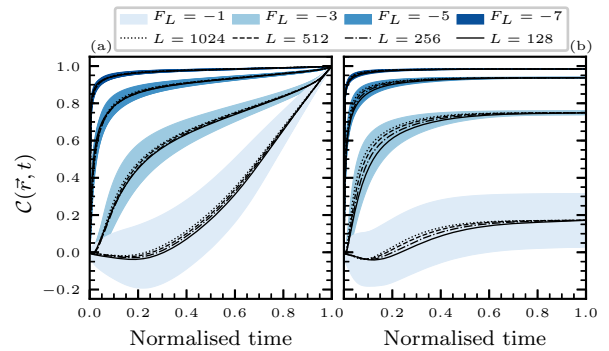


FIG. 2. Spin product correlation functions (black lines with their style indicating the lattice size) at fractional distances F_L (see Eqn. (3)) for periodically bounded lattices of length L , for (a) homogeneous and (b) striped final states. The shaded regions show the standard deviation around the ensemble mean correlation of the largest lattice, shaded according to the fraction of the lattice at which the correlation is measured (Color online). In all cases the correlation show good data collapse between different total system sizes.

compared in normalized time (this is also apparent for product correlations involving higher numbers of spins). In the early time evolution of the system, agreement in the correlations is at its worst particularly for the smallest systems considered. As time progresses or system size increases, correlation values quickly collapse onto universal curves characteristic of the correlation at specified fractional distances. We find that this discrepancy decays rapidly with increasing L , and therefore attribute it to a finite size effect. In order to justify this claim, we compute the difference in equivalent correlations obtained on lattices of lengths separated by a scale factor of $b \geq 2$ such that $L' = bL$. The difference is written as

$$\Delta\mathcal{C}(r, t) = \mathcal{C}(r, t) - \mathcal{C}'(r, t), \quad (4)$$

where \mathcal{C}' is the correlation obtained on the system of length L' at a fractional distance of r at time t . As expected for a finite size effect, the discrepancies rapidly become negligible with increasing system size. Fig. 3 shows this decay for data taken at a single lattice fraction on multiple lattice sizes (the magnitude of the largest discrepancy in $\Delta\mathcal{C}$ being $\approx 25\%$ of the converged value for $L = 32$) for evolution to both stable and metastable final states. Interestingly, the largest discrepancy in the correlations converges from above (below) for stable (metastable) final states.

The dynamic scaling hypothesis asserts that the evo-

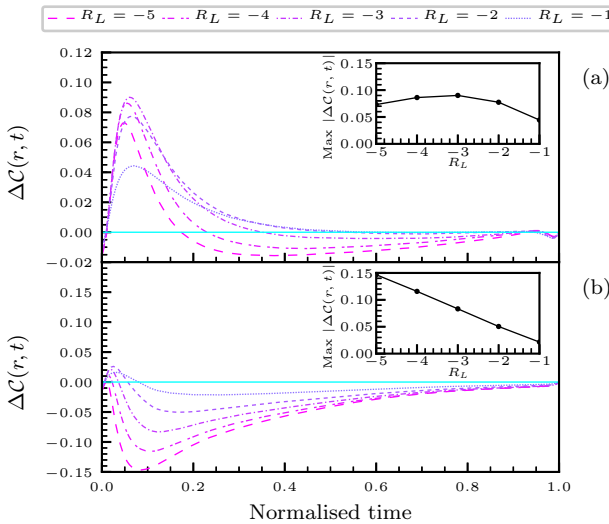


FIG. 3. (Color online) Plots of the differences in equivalent correlations $\Delta\mathcal{C}(r, t)$ between lattice sizes of L and L' for both (a) stable and (b) metastable final state quenches. The correlations used here were measured at lattice fractions of $F_L = -3$. The relative size of the lattices is expressed as $R_L = \log_2(L/L')$. In each case $L' = 1024$, and L varies over $2^5 \leq 2^n \leq 2^9$. The inset plots show the decay in $\max |\Delta\mathcal{C}(r, t)|$. For all the time the maximum differences tend towards zero with increasing system length. The solid horizontal line indicates $\Delta\mathcal{C}(r, t) = 0$.

lution of the system is governed by the growth of a single characteristic length $R_c(T) \propto T^{1/z}$ (where $z = 2$ for the 2D Ising model) [4, 29]. In the regime where this length is greater than the lattice spacing, but smaller than the system length, the two-point correlation functions further collapse onto one universal curve of the form

$$\mathcal{C}(R, T) \propto G\left(\frac{R}{R_c(T)}\right) \propto G\left(\frac{R}{T^{1/z}}\right), \quad (5)$$

at all times. The characteristic length associated with the coarsening process, $R_c(T)$, is a measure of the typical domain size. This can be taken to be the distance at which the two-point correlation functions decays to zero [4]. In the case of the 2D kinetic Ising model the exponent is $z = 2$. Hence spins at shorter distances rapidly correlate and spins at distances longer than the correlation length are essentially uncorrelated. This pattern then extends to longer scales as the system coarsens and domains grow. In the case of finite systems the long time limit of $R_c(T)$ is naturally limited by the system length L (see Fig. 4).

Here we argue that the multiscale equivalence in correlations is of a stronger form, since at all scales and times data collapse of the average of the correlations occur irrespective of the characteristic length scale at a particular time. One may seek to explain this equivalence through two key scaling behaviors of the system. The first of these is the quench time T_q , which for the 2D Ising model is $T_q \propto L^2$ [16] (see Supplemental Material [27]). The second is the growth of the two-point correlation functions in time, which is governed by the dynamical scaling law Eq. 5. There exists compelling numerical evidence for the dynamical scaling description of zero-temperature coarsening in the Ising model [3, 4]. This evidence is generally presented in the form of a universal data collapse when considering the correlations as functions of r/\sqrt{t} [3, 4]. In such studies the distances considered between correlated spins are generally small with respect to the linear dimension of the system, in order to mimic behavior expected in the continuum limit. If the distances at which correlations are measured are extended to a significant fraction of the system length, the finite nature of the system then leads to a breakdown in the expected universal data collapse (see Fig. 4). Even at times where the correlation at larger distances is still low, the spanning domains that determine the final state of the system have emerged, and this affects how the correlations can grow. Interestingly, this effect seems to be different for stable and metastable final state quenches. In the stable final state case, the finite size limitations appear to cause the correlations to grow more slowly, i.e. with an exponent $z > 2$. In the metastable case, the data collapse still fails, but to a lesser extent, until very late times where it is more obvious. At these times the system is close to forming the final striped phase. However, the multiscale equivalence of correlations presented in Fig. 2 holds

not only in the regime where the dynamical scaling description of the zero-temperature coarsening is valid, but also at distances and times where the finite nature of the system is apparent.

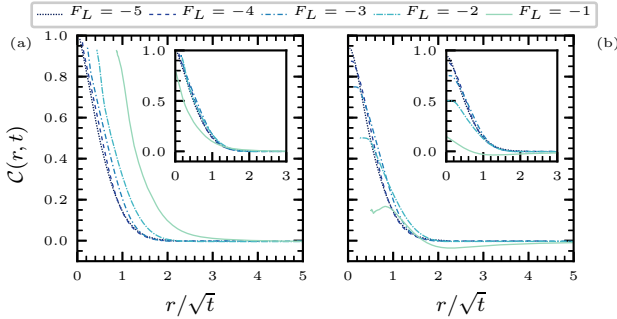


FIG. 4. Shows plots of the correlations as functions of r/\sqrt{t} for (a) stable and (b) metastable final state quenches. In each case the distances considered are relatively large fractions of the system length ($F_L \geq -4$), and the data collapse can be seen to fail. The insets show the same data with a shift in the horizontal axis of $-4(r/L)^2$, i.e. proportional to a dominant domain area, in an attempt restore the data collapse. This is improved for all but the largest lattice fractions. The data is averaged over only the active simulations at each time, and no time value with less than 30 active simulations was used.

In conclusion, we have shown that for finite square lattice Ising ferromagnets evolving under Glauber dynamics, there is an equivalence in how correlations evolve at fractional distances within the system in normalized time that holds for all available length scales across the entire time evolution of the system. Not only does this equivalence exist in the regime where the evolution of the system is well described by the scaling hypothesis describes, but also in the regime where the dynamical scaling description fails due to the finite nature of the system. This suggests the equivalence occurs independently of the characteristic length associated with the coarsening evolution of the system. It would be of interest to see the exploration of this behavior in other systems where the exponent z is the same as the 2D Ising model. Furthermore, there is also scope for investigation in other systems displaying curvature driven coarsening described by different forms of this dynamical scaling law, where the exponent z can vary from system to system, as well as in different regimes of the phase ordering process of a particular system [30].

J.D. acknowledges support from EPSRC DTA grant EP/N509760/1. Results were obtained using ARCHIE-WeSt, EPSRC grant No. EP/K000586/1. The authors would like to thank Oliver Henrich and Sidney Redner for helpful comments during the preparation of this manuscript.

* j.denholm@strath.ac.uk

† benjamin.hourahine@strath.ac.uk

- [1] R. J. Glauber, *Journal of Mathematical Physics* **4**, 294 (1963).
- [2] P. Krapivsky, S. Redner, and E. Ben-Naim, *A Kinetic View of Statistical Physics* (Cambridge University Press, 2010).
- [3] K. Humayun and A. J. Bray, *Journal of Physics A: Mathematical and General* **24**, 1915 (1991).
- [4] A. Bray, *Physica A: Statistical Mechanics and its Applications* **194**, 41 (1993).
- [5] S. Tojo, Y. Taguchi, Y. Masuyama, T. Hayashi, H. Saito, and T. Hirano, *Phys. Rev. A* **82**, 033609 (2010).
- [6] Y. Kawaguchi, H. Saito, K. Kudo, and M. Ueda, *Phys. Rev. A* **82**, 043627 (2010).
- [7] S. De, D. L. Campbell, R. M. Price, A. Putra, B. M. Anderson, and I. B. Spielman, *Phys. Rev. A* **89**, 033631 (2014).
- [8] J. Hofmann, S. S. Natu, and S. Das Sarma, *Phys. Rev. Lett.* **113**, 095702 (2014).
- [9] N. Shitara, S. Bir, and P. B. Blakie, *New Journal of Physics* **19**, 095003 (2017).
- [10] H. Takeuchi, *Phys. Rev. A* **97**, 013617 (2018).
- [11] L. McNally, E. Bernardy, J. Thomas, A. Kalziki, J. Pentz, S. P. Brown, B. K. Hammer, P. J. Yunker, and W. C. Ratcliff, *Nature Communications* **8** (2017).
- [12] B. Skorupa, K. Sznajd-Weron, and R. Topolnicki, *Phys. Rev. E* **86**, 051113 (2012).
- [13] J. Olejarz, P. L. Krapivsky, and S. Redner, *Phys. Rev. E* **83**, 030104 (2011).
- [14] J. Olejarz, P. L. Krapivsky, and S. Redner, *Phys. Rev. E* **83**, 051104 (2011).
- [15] V. Spirin, P. L. Krapivsky, and S. Redner, *Phys. Rev. E* **65**, 016119 (2001).
- [16] V. Spirin, P. L. Krapivsky, and S. Redner, *Phys. Rev. E* **63**, 036118 (2001).
- [17] K. Barros, P. L. Krapivsky, and S. Redner, *Phys. Rev. E* **80**, 040101 (2009).
- [18] J. Olejarz, P. L. Krapivsky, and S. Redner, *Phys. Rev. Lett.* **109**, 195702 (2012).
- [19] U. Yu, *Journal of Statistical Mechanics: Theory and Experiment* **2017**, 123203 (2017).
- [20] L. F. Cugliandolo, *Journal of Statistical Mechanics: Theory and Experiment* **2016**, 114001 (2016).
- [21] T. Blanchard, F. Corberi, L. F. Cugliandolo, and M. Picco, *EPL (Europhysics Letters)* **106**, 66001 (2014).
- [22] C. Godrche and M. Pleimling, *Journal of Statistical Mechanics: Theory and Experiment* **2018**, 043209 (2018).
- [23] P. Mullick and P. Sen, *Phys. Rev. E* **95**, 052150 (2017).
- [24] J. J. Arenzon, A. J. Bray, L. F. Cugliandolo, and A. Sicilia, *Phys. Rev. Lett.* **98**, 145701 (2007).
- [25] F. Corberi, L. F. Cugliandolo, F. Insalata, and M. Picco, *Phys. Rev. E* **95**, 022101 (2017).
- [26] F. M. Bulnes, V. D. Pereyra, and J. L. Riccardo, *Phys. Rev. E* **58**, 86 (1998).
- [27] “See supplemental material,” For other boundary conditions and data extracted from our simulations.
- [28] E. Jones, T. Oliphant, P. Peterson, *et al.*, “SciPy: Open source scientific tools for Python,” (2001–).
- [29] P. C. Hohenberg and B. I. Halperin, *Rev. Mod. Phys.* **49**, 435 (1977).

[30] B. A. Camley and F. L. H. Brown, *J. Chem. Phys.* **135**, 225106 (2011).